An official publication of the International Society for Energy, Environment and Sustainability (ISEES)

Journal of Energy and Environmental Sustainability

Journal homepage : www.jees.in

Comparative analysis of dye decolorization efficiency and growth kinetics of microalgae in the presence of Methyl orange and Rhodamine B dye

Palak Saket[a], Rimjhim Sangtani[a], Dinesh Parida[a], Abhijeet Joshi[a], Kiran Bala[a*]

[a]*Department of Biosciences and Biomedical Engineering, Indian Institute of Technology Indore, Indore, 453552, India*

ARTICLE INFO

Received : 31 January 2024
Revised : 14 May 2024
Accepted : 15 May 2024

Keywords:
Methyl Orange, Rhodamine B, Microalgae, Dye decolorization, Growth kinetics

ABSTRACT

Textile industries are the major contributor to water pollution due to the usage of highly toxic synthetic dyes. Synthetic dyes are non-biodegradable and toxic in nature and, pose significant ecological and health risks. Therefore, this study explores the impact of two prevalent dyes, Rhodamine B (RB) and Methyl Orange (MO), on microalgal growth and their decolorization efficiency. The study reveals differential effects, with RB exhibiting greater toxicity to microalgae compared to MO. Highest biomass growth was observed at 30 and 10 mg/L of MO and RB was 969.5 ± 38.2 µg/mL and 729.9 ± 73.9 µg/L respectively. Moreover, decolorization efficiency was highest in 10 mg/L of dyes, whereas it was highest in the presence of MO dye (54.6 ± 1.3%) compared to RB. Microscopic and spectroscopic analyses provide insights into morphological changes and surface interactions between microalgae and dyes. These findings underscore the potential of microalgae in dye removal, with implications for wastewater treatment and by-product generation.

© 2024 ISEES, All rights reserved

1. Introduction

Industrialization is one of the primary reasons for the economic wealth of any country. Industries such as textile industries utilize a massive amount of fresh water during the process of dyeing. Moreover, these industries are one of the significant contributors to water pollution due to the presence of dye. It contributes to releasing 54% of dyes among other dye-utilizing industries like paint, paper, and dye manufacturers [Katheresan et al., 2018]. Yearly consumption of dyes by textile industries is approximately 700000 tonnes. After the process of dyeing, the remaining colorants are released into the ecosystem without any prior treatment [Salima et al., 2013]. It is estimated that 200,000 tonnes of dye effluents are released into the water bodies per year from textile industries worldwide [Piaskowski et al., 2018]. These dyes are non-biodegradable in nature, carrying aromatic ring structures, making them more complex to degrade. They have highly toxic effects on phytoplankton, as they prevent the penetration of light, which affects the photosynthesis process, thereby causing a reduction in the metabolic functioning of aquatic plants and animals [Samchetshabam et al., 2017]. The human body is also exposed to dyes through the food chain. Acute exposure to these dyes has mutagenic and carcinogenic effects [Sarkar et al., 2017]. Moreover, in dry or wet form, when in contact with the skin, these dyes can lead to allergic reactions [Akarslan and Demiralay, 2015]. Synthetic dyes contain a chromophore attached to ring structure and aromatic amines, which makes the degradation of synthetic dyes challenging [Wu et al., 2020]. These dyes are more harmful as they degrade to toxic by-products. Rhodamine B (RB) is a cationic dye, and Methyl Orange (MO) is an anionic dye known to be the most hydrophilic dye existing in the aquatic ecosystem [Bhowmik et al., 2018]. The 1 mg/L textile dye concentration in water can potentially threaten human and aquatic health [Adegoke et al., 2022]. RB, being the basic dye composed of complex xanthene structures, binds strongly into the chromophore clusters. Therefore, it exhibits high stability in water for a much longer time [Fatimah et al., 2022]. RB dye is known to be used in numerous fields, such as plastic, textile, paper, leather, glass painting, cloth painting, etc. [Al-Gheethi et al., 2022]. On the other hand, MO, being the sulfonated dye, has a lower rate of fixation on the substrate during dyeing and a higher rate of desorption, thus getting released into the water stream. MO, being highly water soluble and stable, is used extensively in manifold industries such as leather, paper, tanning, cosmetics, textile, food, etc [Bhowmik et al., 2020]. Due to the presence of the benzidine group in the chemical structure, MO exhibits a highly toxic nature, even in case of contact, inhalation, or swallowing [Pillai, 2017]. These dyes have multiple ring structures, which makes their degradation processes more complex and ineffective for aerobic digestion. They carry mutagenic and carcinogenic groups [Afkhami and Moosavi, 2010]. Therefore, the effective and efficient degradation of dye is very challenging [Khalaf, 2008].

Primitive and traditional techniques developed for removing dyes from wastewater include ozonization, flocculation, photocatalytic degradation, and membrane separation [Liang et al., 2017]. These processes have disadvantages like high cost, chemically more toxic by-products, and sludge

*Corresponding Author: *kiranb@iiti.ac.in*

© 2024 ISEES, All rights reserved

formation [Kaushik and Malik, 2009]. Since synthetic dyes are ineffective in photodegradation and oxidation, they are unable to self-degrade with time. Therefore, in recent times, the focus has been more on designing biological techniques for dye degradation and their removal with the least limitations. Microalgae have proven to be more promising in removing dyes because of less chance of toxic by-product formation, and the residual biomass can serve as a potential source for biofuel production [Baldev et al., 2013]. In response to dyes, the live microalgae cells perform extracellular and intracellular enzymatic degradation mechanisms for their removal [Hernández-Zamora et al., 2015]. This allows the alteration of the original structure of the dye and mineralization into a non-toxic form [Ali, 2010]. Baldev and colleagues studied the decolorization of Rhodamine B by *Coelastrella* sp. and showed 80% removal of dye and its conversion to a non-toxic form [Baldev et al., 2013]. *Chlorella vulgaris,* in the presence 25 mg/L concentration of Congo red, was able to remove 58% of the dye through biosorption and biodegradation. The removal capacity of algae depends on the concentration and chemical structure of dyes along with the experimental conditions [Hernández-Zamora et al., 2015]. Different microalgal species have been explored for their dye decolorization efficiency in the past decade, but very few studies have focused on the growth kinetics and other biochemical properties of microalgae, to target the biorefinery approach. Microalgae have been known to treat wastewater along with the production of different bioproducts such as biofuels, biopolymers, etc.The significance of the current study is to unravel the tolerance of native microalgal species and to compare the effect of two extensively utilized and complex dyes, MO, and RB, on the growth and morphology of microalga. The study also investigated the decolorization efficiency of microalga when exposed to the anionic (MO) and cationic (RB) dye independently. UV-visible spectroscopy, FTIR spectroscopy, and scanning electron microscopy we aim to compare RB and MO dye in term of their decolorization and their effect on microalgal growth kinetics.

2. Materials and Methods

2.1 Chemicals

BG-11 media, MO, and RB dye were purchased from HI Media Pvt. Ltd. (India). HCl and NaOH were purchased from Merck (India) to maintain pH.

2.2 Microalgal culture conditions

Microalgae *Scenedesmus* sp. was isolated and purified from nearby regions of Indore, M.P. BG-11 media was used to cultivate and maintain indigenous *Scenedesmus* sp. stock culture by providing optimum light and temperature conditions in the culture room. The conditions of the culture room were maintained at the light intensity of 3000 ± 500 lux of white, fluorescent light, at a temperature of 27 ± 5 C, and light: dark photoperiod of about 12:12.

2.3 Microalgal cell growth kinetics

The biomass concentration produced was calculated by considering the linear equation obtained from the optical density (OD_{680nm}) vs. cell dry weight standard curve. Further, the cell growth kinetics was determined by calculating biomass productivity, specific growth rate, and doubling time from biomass concentration and optical densities as adapted from [Guillard, 1973; Pancha et al., 2015] depicted in the following equations:

$$Biomass\ Productivity\left(\mu\frac{\frac{g}{mL}}{Day}\right), P = \frac{(X_2 - X_1)}{(T_2 - T_1)} \quad (1)$$

X_2 and X_1 are the concentrations of algal biomass at time T_2 and T_1 respectively.

$$Specific\ Growth\ Rate\ (per\ Day), \mu = \frac{ln\frac{N_t}{N_0}}{T_t - T_0} \quad (2)$$

where, N_t and N_0 indicates OD_{680nm} observed at time T_t and T_0 respectively.

$$Division\ Time = \frac{0.69}{\mu} \quad (3)$$

Here μ the specific growth rate.

2.4 Dye decolorization efficiency

The samples from the culture medium were collected and centrifuged every alternate day. The supernatant was collected and subjected to absorbance recording using spectrophotometric analysis. Dye decolorization efficiency was determined by a standard calibration curve. The calibration curve was prepared by scanning a solution of MO and RB dye in the UV-Vis range of 200-800 nm, and λ_{max} was selected for taking absorbance of samples for calculation of decolorization efficiency. The decolorization efficiency was calculated by following the equation [Daneshvar et al., 2007].

where, C_0 - initial dye concentration in mg/L, C- final dye concentration in mg/L.

2.5 Fourier Transform Infrared (FTIR) Spectroscopy

The 10th day lyophilized biomass was subjected to FTIR analysis. FTIR was conducted in Tensor 27, BRUKER with KBr beam splitter and Mid IR source zinc selenium, having detector DLaTGS. Pellets of samples were prepared with KBr and subjected to FTIR analysis within the scan range of 4000 cm^{-1} to 400 cm^{-1} [Yan and Pan, 2004].

2.6 Scanning Electron Microscopy (SEM)

For visualization of the morphology of dye-treated samples, 10th-day culture samples were treated with a series of ethanol concentrations, a slide was prepared by the drop-cast method, and SEM analysis was performed by using Supra 55 Zeiss FE-SEM [Kishor et al., 2021].

2.7 Experimental setup

Exponentially growing cells of *Scenedesmus* sp. were used for inoculation in batch cultures with initial optical density 0.5 (OD_{680nm}) and 10, 30, 50, 70, and 100 mg/L concentrations as initial MO and RB dye concentrations. 100 mL culture volume was taken in 250 mL flasks for performing the experiment. The experiment was performed in triplicates. The experimental conditions were provided as follows: 3000 ± 500 lux at 27 ± 5 C and 12:12 photoperiod. The pH of the solution was maintained to be 7.5 with 1N NaOH and 1N HCl with the help of a pH meter (Systronics pH System 361). The experiment was set in manual shaking conditions twice a day to avoid sticking cells in the bottom of the flasks. The growth of the cells was monitored every alternate day by recording OD at 680 nm on a spectrophotometer (Hach DR 6000). OD was recorded after several washing of cells with autoclaved distilled water. The cells were centrifuged, and the supernatant was used to take the absorbance of dyes. The absorbance of dyes in media was recorded at specific wavelengths (554 nm for RB and 466 nm for MO) on every alternative day. The algal cells exposed to MO dye ($Algae_{MO}$) and RB dye ($Algae_{RB}$) were harvested on the 10th day, where maximum decolorization was observed, and the biomass was collected for FTIR and SEM evaluation.

3. Results and Discussion

3.1 Impact of dyes on the growth and biomass of microalgae

Scenedesmus sp. was subjected to different initial dye concentrations (10, 30, 50, 70, 100 mg/L) of two dyes, *i.e.*, MO and RB. The experiment was performed in triplicates. The biomass yield (μg/mL) in $Algae_{MO}$ and $Algae_{RB}$ in different concentrations of dye is shown in Figure 1. In $Algae_{MO}$, the *Scenedesmus* sp. inoculated with 30 mg/L dye reached a maximum biomass yield of 969.5 ± 38.25 μg/mL on the 10th day of the incubation (Figure 1A). Meanwhile, biomass concentration was lower in the presence of other initial concentrations of MO (10, 20, 50, 70, and 100 mg/L). On the other hand, in the presence of RB, the maximum biomass yield observed was 792.9 ± 73.9 μg/mL in $Algae_{RB}$ of 10 mg/L dye concentration on the 10th day (Figure 1B), which was higher compared from other initial concentrations of RB (20, 30, 50, 70 and 100 mg/L). This indicates that RB was more toxic to microalgae than MO. Besides this, 30 mg/L and 10 mg/L initial concentrations of MO and RB, respectively, were favourable enough for microalgal growth. The data analysis demonstrated that microalgae growth was not completely hampered when subjected to different concentrations of both dyes till the 10th day of incubation; however, after the 10th day, growth and decolorization efficiency were not evidently varying. Therefore, the microalgal cells were incubated with dyes for up to 10 days. Interestingly, the presence of RB dye in the media affected the growth of microalgae more distinctly than the

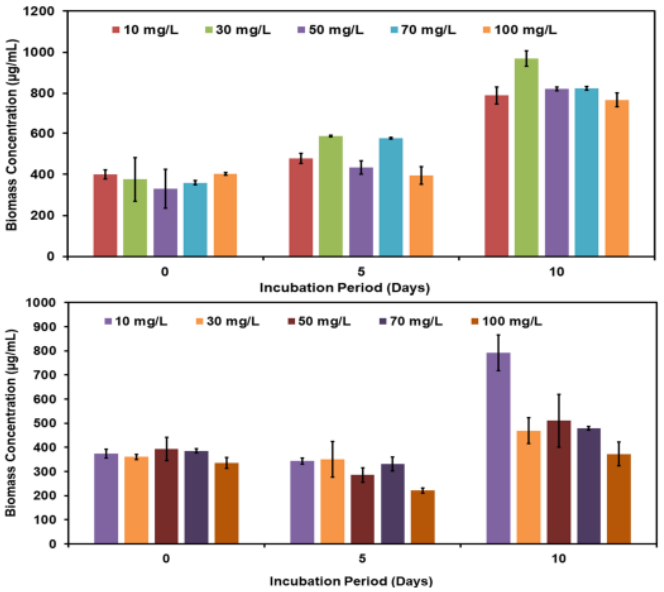


Figure 1. Biomass concentration of Scenedesmus sp. on different incubation days when exposed to different concentrations of dyes (A). $Algae_{MO}$ and (B). $Algae_{RB}$

presence of MO. In $Algae_{MO}$, the biomass concentration of *Scenedesmus* sp. in 100 mg/L MO (768.2 ± 33.4 µg/mL) was found to be 2-fold high as compared to the biomass in 100 mg/L RB in $Algae_{RB}$ (373.1 ± 49.8 µg/mL) on 10th day. It was also observed that microalgae growth was slower in the presence of RB than MO, as evident from the biomass yield on the 5th and 10th day and from the growth kinetics, as depicted in Table 1.

While comparing the cell growth kinetics of $Algae_{MO}$ and $Algae_{RB}$ on the 10th day, the specific growth rate, biomass productivity, and doubling time of $Algae_{MO}$ at a concentration of 30 mg/L was 71.9 ± 15.4 µg/mL/day, 0.09 per day, and 7.6 days, respectively. The cell growth kinetics suggested that the microalgal cells were growing and dividing very efficiently in the presence of $Algae_{MO}$ at 30 mg/L. However, higher concentrations affected the growth of *Scenedesmus* sp., as evidenced by different growth factors. In comparison to $Algae_{MO}$, the growth kinetic parameters of $Algae_{RB}$ were either negative or varied drastically, as shown in Table 1, thus indicating the toxic effect of RB on cell function and growth. Moreover, the structure of MO is simpler than that of RB as it has 2 benzene rings, whereas RB has 4 benzene rings. Therefore, the enzymatic breakdown of MO dye was easier for microalgae than RB dye. That is why biomass growth was hampered more in the lowest RB dye concentration than in MO. In contrast, the growth of the algal biomass was promoted by the MO dye molecule and its metabolites, which worked as the source of carbon and nitrogen for microalgae (Kishor et al., 2021; Saratale et al., 2009). Hence, it can be assumed that the initial concentration of 30 mg/L of MO acted as survivable feed for microalgae, which can easily break down MO dye into simpler forms and promote an increase in biomass concentration. However, in 10 mg/L, the initial concentration of MO dye was tolerable, but due to insufficient formation of metabolites, it couldn't support the increment in biomass concentration. Therefore, it can be concluded that the increase in the dye concentrations has a negative influence on microalgal metabolism, which agrees with previous results obtained from the literature [Acuner and Dilek, 2004]. In previous findings, it has been observed that the major reason behind the inhibition of microalgal growth could be due to the incorporation of dye molecules between the base pairs of DNA, thus making the double helix stable. This stabilization further obviates the base pair separation and enzyme activity and restricts cell replication [Hernández-Zamora et al., 2014].

3.2 Evaluation of dye decolorization efficiency of Scenedesmus sp.

The dye decolorization percentage in $Algae_{MO}$ and $Algae_{RB}$ has been shown in Figure 2. Dye decolorization efficiency was observed for different dye

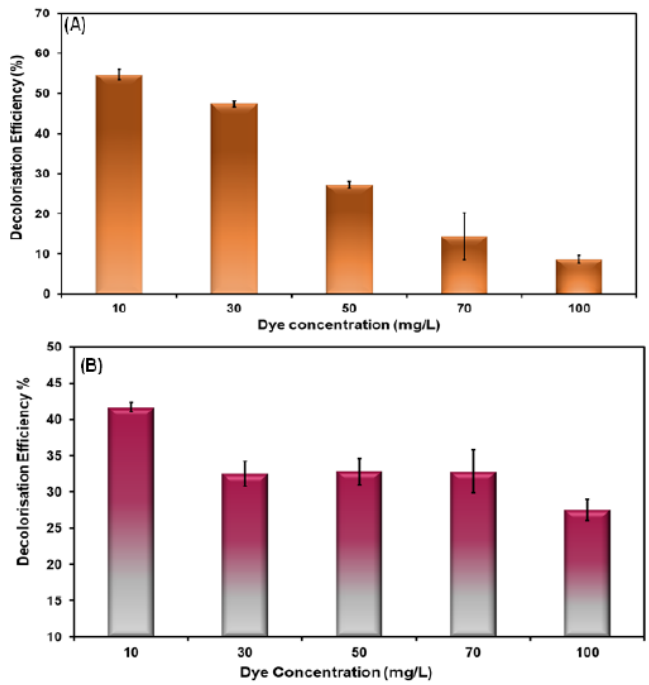


Figure 2. Dye decolorization efficiency of Scenedesmus sp. on the 10th day after exposure to different concentrations of dyes (A). $Algae_{MO}$ and (B). $Algae_{RB}$

Table 1. Microalgal cell growth kinetic parameters in the presence of MO and RB dye

Growth kinetic parameters in $Algae_{MO}$						
Dye concentration (mg/L)	**Biomass Productivity (µg/mL/Day)**		**Specific Growth Rate (per Day)**		**Division Time (Days)**	
	Day 5	**Day 10**	**Day 5**	**Day 10**	**Day 5**	**Day 10**
10	15.3 ± 3.3	38.9 ± 1.3	0.03	0.06	22.5	11.0
30	36.3 ± 2.3	71.9 ± 15.4	0.07	0.09	9.5	7.6
50	21.6 ± 0.7	49.3 ± 5.04	0.05	0.09	13.2	8.1
70	45.4 ± 0.0	58.5 ± 18.2	0.1	0.08	7.5	9.1
100	NA	40.6 ± 0.00	NA	0.07	NA	10.4
Growth kinetic parameters in $Algae_{RB}$						
10	NA	41.8 ± 9.2	NA	0.07	NA	10.30
30	1.0 ± 0.2	4.7 ± 0.01	0.01	0.01	297.1	63.2
50	NA	11.9 ± 4.2	NA	0.02	NA	32.4
70	NA	8.7 ± 0.01	NA	0.02	NA	37.8
100	NA	0.9 ± 0.1	NA	NA	NA	NA

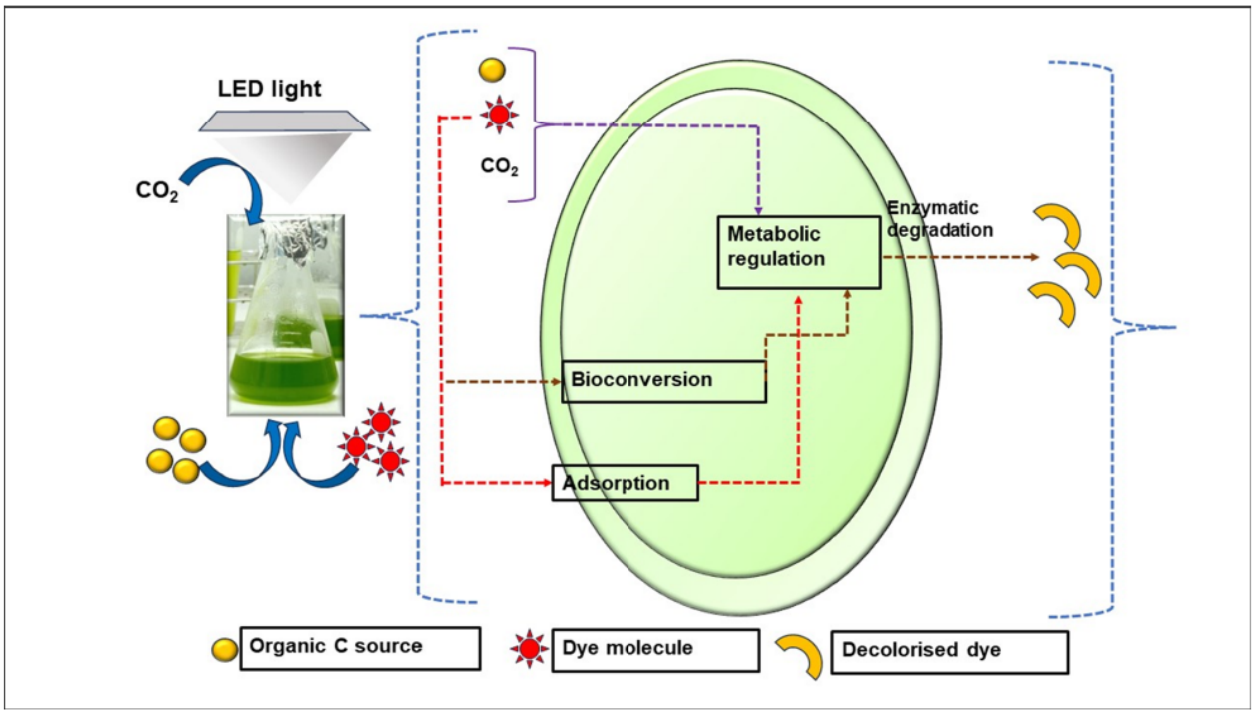


Figure 3. Decolorization mechanism adopted by microalgae for removal of dye

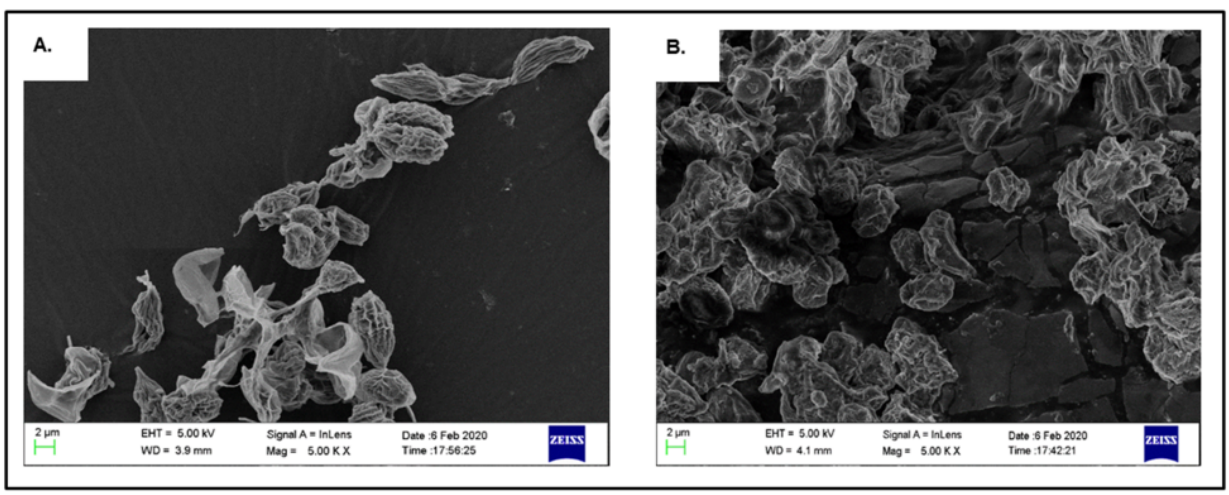


Figure 4. Scanning electron micrographs of (A). $Algae_{MO}$ and (B). $Algae_{RB}$

concentrations on different incubation periods. It was determined that the highest removal of both dyes was obtained on the 10^{th} day in $Algae_{MO}$ and $Algae_{RB}$. In the case of $Algae_{MO}$, a maximum decolorization efficiency of 54.6 ± 1.3 % was observed for 10 mg/L dye, followed by 47.3 ± 0.82 % for 30 mg/L, and the same trend was observed for other concentrations, *i.e.*, with increasing concentration of dye, the dye decolorization efficiency was getting reduced. Whereas $Algae_{RB}$, the maximum decolorization percentage was observed at 10 mg/L (41.6 ± 0.64 %), the lowest decolorization for 100 mg/L (27.5 ± 1.4%). However, stable RB decolorization efficiency was observed at 30 to 70 mg/L. This could be because, in these initial concentrations (30, 50, 70 mg/L), the biomass concentration was also similar on the 10th day (Figure 1(B)), which maintained a stable decolorization efficiency. However, at 100 mg/L initial concentration, decolorization efficiency significantly decreased owing to a decrease in biomass concentration. While comparing the difference in the decolorization of the dyes, the higher removal of MO might be credited to the presence of the sulfonic charged group in the vicinity of an azo group in the molecular structure of dye, which acts via resonance as an electron-withdrawing group and leads to increase in the color removal for enhanced decolorization [Hsueh and Chen, 2007]. Whereas, in the case of RB, the cells experienced stress and were not able to resist the effect of RB, consisting of complex molecular structures. In a recent study, photocatalytic degradation of MO dye by Mn_3O_4-based nanocomposites reported 95.5% removal of dye from 20 mg/L of initial concentration (Osgouei et al., 2020). In addition, 82.14% removal of RB dye was reported by Xu et al., 2021 via ultrasound-assisted TiO_2-based photocatalysis (Xu & Ma, 2021). Glutaraldehyde and polyvinyl alcohol crosslinked cellulose membrane was studied for MO removal, and 93.5% dye removal from 10 mg/L initial concentration was reported (Hou et al., 2019). Moreover, a study conducted on polyethylene glycol-tannic acid-based membrane filtration of 5 mg/L of RB dye reported 98.9% RB removal from the aqueous solution (Shi et al., 2018). These reported techniques can efficiently (>80%) remove MO and RB dye from the solution. Methods like photocatalytic degradation and membrane separation consume chemicals for membrane preparation and effective metals for photocatalytic activity, which brings the cost to the method. However, in the current study, 50% of dye removal was achieved by microalgae, and the residual biomass can be utilized for by-product

generation, hence it can bring the cost down, for this method, and the efficiency of microalgae can be increased by optimizing the physiochemical parameters (Ghosh et al., 2020) for enhancing dye removal efficiency and biomass production.

Furthermore, reason for reduced decolorization efficiency at higher concentrations of dyes could be the inhibition of enzyme activity, which reduced cellular functions due to the toxic and negative impact of higher dye concentration. On the other hand, while comparing the algal growth in $Algae_{RB}$, it was observed that though the production of algal biomass with increasing concentration was less, the decolorization efficiency with increasing dye concentration was still not affected much. Thus, it implies that the mechanism adopted by microalgae for decolorization might be the rapid removal via the utilization of non-living algal cells for the adsorption of dye molecules and a similar phenomenon has also been discussed in previous studies [Elgarahy et al., 2023].

As per the previous studies, algae have been known to employ three distinct dye decolorization mechanisms, including chromophore adsorption by algal biomass, degradation of azo dyes facilitated by the expression of enzyme azo reductase, and consumption of dye chromophores as a nutrient and inducing the conversion of colored compounds into de-colored compounds, for enhancing algal biomass production. In addition, the chemical structure and concentration of dye, along with the physicochemical characteristics of microalgae, play a vital role in determining the mechanism employed by microalgae for the decolorization of dye [Saket et al., 2022]. This phenomenon of the decrease in dye decolorization efficiency with increment in dye concentration was also reported by [Baldev et al., 2013]. A mechanism for dye decolorization by microalgae is depicted in Figure. 5.

3.3 Microscopic visualization of microalgae and dye interaction

Changes in the morphology of microalgal cells were due to the exposure of dye, and electron microscopy, i.e., SEM, was performed to examine the changes in the microalgal surface morphology and topology. As shown in Figure 4, in $Algae_{MO}$ (Figure 4A) and $Algae_{RB}$ (Figure 4B), the algal cells were observed to be rough, irregular, and ruptured with grooves and depressions on the surface as compared the micrographs shown by (Mosleh et al., 2021; Tripathi et al., 2015). The cells were reduced in size; even the cell shape was not oval and elongated from the edges. The similar effect of the dye exposure on the microalgal cells has also been discussed in previous research studies [da Rosa et al., 2018]. Thus, exposure of microalgal cells to dye affected not only their metabolism but also their physiological and morphological appearances.

3.4 FTIR analysis

To investigate the role of microalgal surface interaction with MO and RB dye, FTIR analysis was performed. Figure 5 indicates the FTIR spectra of microalgal biomass of $Algae_{MO}$ and $Algae_{RB}$. However, the FTIR spectra of pristine *Scenedesmus* sp. are discussed by Kashyap et al. 2021 (Kashyap et al., 2021) and reported the appearance of peaks belonging to the following functional groups: amides (N-H), carbohydrates (CH_2 and CH_3), hydroxyl group (O-H), and carboxyl (COO^-) groups. A prominent difference in the intensities of certain peaks compared to (Kashyap et al., 2021) has been observed in $Algae_{MO}$ and $Algae_{RB}$ in the present study, indicating the involvement of functional groups in the formation of bonds with MO and RB dye molecules, and a comparison has been made. For example, the peak at 2915.91 cm^{-1} control biomass attributed to O-H stretching vibration of the carboxyl group [Dittert et al., 2012] has been observed to be shifted to 2927.77 cm^{-1} and 2921.99 cm^{-1} in $Algae_{MO}$ and $Algae_{RB}$. The peak at 2846.86 cm^{-1}, denoted to C-H stretching in the carboxylic group, shifted to 2858.34 cm^{-1} and 2852.55 cm^{-1} in AlgaeMO and AlgaeRB, respectively. In addition, the peak at 1621.22 cm^{-1}, which corresponds to amide and aldehydes groups [Silverstein and Bassler, 1963], has been shifted to 1664.47 cm^{-1} and 1656.75 cm^{-1} in AlgaeMO and AlgaeRB, respectively. Similarly, peaks at 1539.83 cm^{-1}, 1033.36 cm^{-1}, and 1241.55 cm^{-1}, which corresponds to the carboxylic group (C=O) [Dittert et al., 2012], bending of methyl lipid and carboxylic acid also shifted to different wavenumbers in $Algae_{MO}$ and $Algae_{RB}$. All these bands are observed to be different in intensity in both $Algae_{MO}$ and $Algae_{RB}$. This is due to the formation of an electron cloud when an ion is attached to the functional group, which results in a decrease in the density of the electron along with an increase in bond length, which further results in a change in intensity and broadness of a peak [Elangovan et al., 2008].

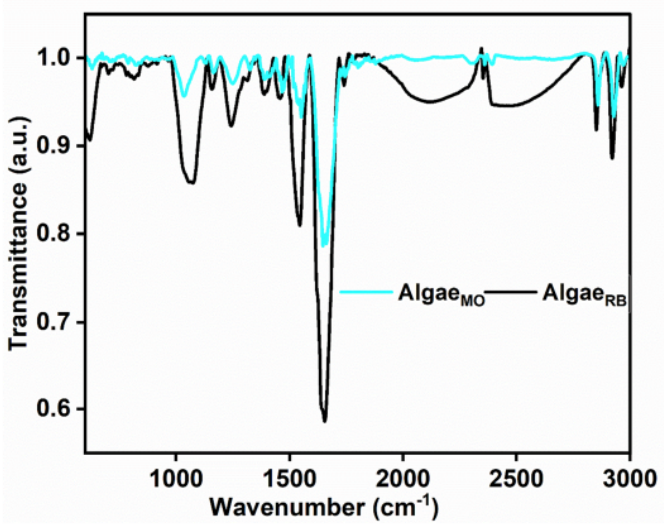


Figure 5. FTIR analysis of $Algae_{MO}$ and $Algae_{RB}$

4. Conclusions

The investigation determined the comparative dye decolorization efficiency as well as the tolerant capacity of *Scenedesmus* sp. Apart from that, it also validated the fact that indigenous microalgae have the potential to decolorize different synthetic dyes with different molecular weights, chemical structures, and polarities. *Scenedesmus* sp. showed the highest biomass growth in the presence of 30 mg/L MO dye. *Scenedesmus* sp. showed the highest decolorization efficiency for 10 mg/L concentration of both the dyes. A comparative SEM analysis was also performed to validate the toxic effects of both dyes on the microalgae via visualizing the surface morphology of microalgal cells. The results not only corroborated interesting observations regarding the mitigation of dyes but also showed that natively isolated *Scenedesmus* sp. has the potential to remediate different types of dyes in optimized lab-scale conditions. Hence, more investigations can warrant better decolorization efficiency and removal of these dyes.

Ethics approval

Not applicable.

Consent for publication

All the authors have seen this paper and given their consent to publish in JEES.

Competing interest

Authors declare that they do not have any personal or financial conflicts of interest.

Funding

MOES (Ministry of Earth Sciences) (MOES/16/19/2017-RDEAS).

Authors' contributions

PS: Methodology, Conceptualization, Formal Analysis, Writing-Original Draft Preparation, **RS**: Formal Analysis, Writing- Reviewing and Editing, **DP**: Formal Analysis, Writing-Reviewing and Editing **AJ**: Supervision, Validation, **KB**: Supervision, Validation, Resources.

Acknowledgments

PS, RS, and DP would like to acknowledge financial support from UGC and SIC IIT Indore for the instrumentation facility. KB is thankful to Ministry of Earth Sciences for financial support. Authors would like to acknowledge IIT Indore for encouraging and providing research facilities.

References

1 Acuner, E., Dilek, F.B., 2004. Treatment of tectilon yellow 2G by *Chlorella vulgaris*. Process Biochem 39, 623–631. https://doi.org/10.1016/S0032-9592(03)00138-9

2 Adegoke, K.A., Adegoke, O.R., Araoye, A.O., Ogunmodede, J., Agboola, O.S.,

Bello, O.S., 2022. Engineered raw, carbonaceous, and modified biomass-based adsorbents for Rhodamine B dye removal from water and wastewater. Bioresour Technol Rep 18, 101082. https://doi.org/10.1016/j.biteb.2022.101082

3 Afkhami, A., Moosavi, R., 2010. Adsorptive removal of Congo red, a carcinogenic textile dye, from aqueous solutions by maghemite nanoparticles. J Hazard Mater 174, 398–403. https://doi.org/10.1016/j.jhazmat.2009.09.066

4 Akarslan, F., Demiralay, H., 2015. Effects of Textile Materials Harmful to Human Health. Acta Phys Pol A 128, B-407-B-409. https://doi.org/10.12693/APhysPolA.128.B-407

5 Al-Gheethi, A.A., Azhar, Q.M., Senthil Kumar, P., Yusuf, A.A., Al-Buriahi, A.K., Radin Mohamed, R.M.S., Al-shaibani, M.M., 2022. Sustainable approaches for removing Rhodamine B dye using agricultural waste adsorbents: A review. Chemosphere 287, 132080. https://doi.org/10.1016/j.chemosphere.2021.132080

6 Ali, H., 2010. Biodegradation of Synthetic Dyes—A Review. Water Air Soil Pollut 213, 251–273. https://doi.org/10.1007/s11270-010-0382-4

7 Baldev, E., MubarakAli, D., Ilavarasi, A., Pandiaraj, D., Ishack, K.A.S.S., Thajuddin, N., 2013. Degradation of synthetic dye, Rhodamine B to environmentally non-toxic products using microalgae. Colloids Surf B Biointerfaces 105, 207–214. https://doi.org/10.1016/j.colsurfb.2013.01.008

8 Bhowmik, M., Debnath, A., Saha, B., 2020. Fabrication of mixed phase $CaFe_2O_4$ and $MnFe_2O_4$ magnetic nanocomposite for enhanced and rapid adsorption of methyl orange dye: statistical modeling by neural network and response surface methodology. J Dispers Sci Technol 41, 1937–1948. https://doi.org/10.1080/01932691.2019.1642209

9 Bhowmik, M., Debnath, A., Saha, B., 2018. Fabrication of mixed phase calcium ferrite and zirconia nanocomposite for abatement of methyl orange dye from aqua matrix: Optimization of process parameters. Appl Organomet Chem 32. https://doi.org/10.1002/aoc.4607

10 Dotto, G.L., Sander, H., Feris, L.A., 2018. Biosorption of rhodamine B dye from dyeing stones effluents using the green microalgae *Chlorella pyrenoidosa*. J Clean Prod 198, 1302–1310. https://doi.org/10.1016/j.jclepro.2018.07.128

11 Dittert, Ingrid M., Vilar, V.J.P., da Silva, E.A.B., de Souza, S.M.A.G.U., de Souza, A.A.U., Botelho, C.M.S., Boaventura, R.A.R., 2012. Adding value to marine macro-algae *Laminaria digitata* through its use in the separation and recovery of trivalent chromium ions from aqueous solution. J. Chem. Eng. 193–194, 348–357. https://doi.org/10.1016/j.cej.2012.04.048

12 Elangovan, R., Philip, L., Chandraraj, K., 2008. Biosorption of hexavalent and trivalent chromium by palm flower (*Borassus aethiopum*). J. Chem. Eng 141, 99–111. https://doi.org/10.1016/j.cej.2007.10.026

13 Elgarahy, A.M., Maged, A., Elwakeel, K.Z., El-Gohary, F., El-Qelish, M., 2023. Tuning cationic/anionic dyes sorption from aqueous solution onto green algal biomass for biohydrogen production. Environ Res 216, 114522. https://doi.org/10.1016/j.envres.2022.114522

14 Ghosh, A., Samadhiya, K., Kashyap, M., Anand, V., Sangwan, P., & Bala, K. (2020). The use of response surface methodology for improving fatty acid methyl ester profile of Scenedesmus vacuolatus. *Environmental Science and Pollution Research*, *27*, 27457–27469. https://doi.org/10.1007/s11356-019-07115-5

15 Purwiandono, G., Hidayat, A., Sagadevan, S., Kamari, A., 2022. Mechanistic insight into the adsorption and photocatalytic activity of a magnetically separable □-Fe2O3/Montmorillonite nanocomposite for rhodamine B removal. Chem Phys Lett 792, 139410. https://doi.org/10.1016/j.cplett.2022.139410

16 Guillard, R., 1973. Division rates. Handbook of Phycological Methods□ : Culture Methods and Growth Measurements.

17 Hernández-Zamora, M., Cristiani-Urbina, E., Martínez-Jerónimo, F., Perales-Vela, H.V., Ponce-Noyola, T., Montes-Horcasitas, M. del C., Cañizares-Villanueva, R.O., 2015. Bioremoval of the azo dye Congo Red by the microalga *Chlorella vulgaris*. Environ. Sci. Pollut. Res. 22, 10811–10823. https://doi.org/10.1007/s11356-015-4277-1

18 Hernández-Zamora, M., Martínez-Jerónimo, F., 2019. Exposure to the azo dye Direct blue 15 produces toxic effects on microalgae, cladocerans, and zebrafish embryos. Ecotoxicology 28, 890–902. https://doi.org/10.1007/s10646-019-02087-1

19 Hernández-Zamora, M., Perales-Vela, H.V., Flores-Ortíz, C.M., Cañizares-Villanueva, R.O., 2014. Physiological and biochemical responses of *Chlorella vulgaris* to Congo red. Ecotoxicol Environ Saf 108, 72–77. https://doi.org/10.1016/j.ecoenv.2014.05.030

20 Hsueh, C.-C., Chen, B.-Y., 2007. Comparative study on reaction selectivity of azo dye decolorization by *Pseudomonas luteola*. J Hazard Mater 141, 842–849. https://doi.org/10.1016/j.jhazmat.2006.07.056

21 Hou, T., Guo, K., Wang, Z., Zhang, X.-F., Feng, Y., He, M., & Yao, J. (2019). Glutaraldehyde and polyvinyl alcohol crosslinked cellulose membranes for efficient methyl orange and Congo red removal. *Cellulose*, *26*, 5065–5074. https://doi.org/10.1007/s10570-019-02433-w

22 Katheresan, V., Kansedo, J., Lau, S.Y., 2018. Efficiency of various recent wastewater dye removal methods: A review. J Environ Chem Eng 6, 4676–4697. https://doi.org/10.1016/j.jece.2018.06.060

23 Kashyap, M., Samadhiya, K., Ghosh, A., Anand, V., Lee, H., Sawamoto, N., Ogura, A., Ohshita, Y., Shirage, P. M., & Bala, K. (2021). Synthesis, characterization and application of intracellular Ag/AgCl nanohybrids biosynthesized in Scenedesmus sp. as neutral lipid inducer and antibacterial agent. *Environmental Research*, *201*, 111499. https://doi.org/10.1016/j.envres.2021.111499

24 Kaushik, P., Malik, A., 2009. Fungal dye decolourization: Recent advances and future potential. Environ Int 35, 127–141. https://doi.org/10.1016/j.envint.2008.05.010

25 Khalaf, M., 2008. Biosorption of reactive dye from textile wastewater by non-viable biomass of *Aspergillus niger* and *Spirogyra* sp. Bioresour Technol 99, 6631–6634. https://doi.org/10.1016/j.biortech.2007.12.010

26 Kishor, R., Purchase, D., Saratale, G.D., Ferreira, L.F.R., Bilal, M., Iqbal, H.M.N., Bharagava, R.N., 2021. Environment friendly degradation and detoxification of Congo red dye and textile industry wastewater by a newly isolated *Bacillus cohnni* (RKS9). Environ Technol Innov 22, 101425. https://doi.org/10.1016/j.eti.2021.101425

27 Kishor, R., Purchase, D., Saratale, G. D., Ferreira, L. F. R., Hussain, C. M., Mulla, S. I., & Bharagava, R. N. (2021). Degradation mechanism and toxicity reduction of methyl orange dye by a newly isolated bacterium Pseudomonas aeruginosa MZ520730. *Journal of Water Process Engineering*, *43*, 102300. https://doi.org/10.1016/j.jwpe.2021.102300

28 Liang, J., Xia, J., Long, J., 2017. Biosorption of methylene blue by non-living biomass of the brown macroalga *Sargassum hemiphyllum*. Water Sci. Technol. 76, 1574–1583. https://doi.org/10.2166/wst.2017.343

29 Mahajan, P., Kaushal, J., 2020. Phytoremediation of azo dye methyl red by macroalgae *Chara vulgaris* L.: kinetic and equilibrium studies. Environ. Sci. Pollut. Res. 27, 26406–26418. https://doi.org/10.1007/s11356-020-08977-w

30 Mosleh, Y., Mofeed, J., Nafea, E.-S., & Heham, S. (2021). Use of the microalga Scenedesmus obliquus (Turpin) Kutzing to remove some heavy metals from the industrial wastewaters. *Egyptian Journal of Aquatic Biology & Fisheries*, *25*(5).

31 Osgouei, M. S., Khatamian, M., & Kakili, H. (2020). Improved visible-light photocatalytic activity of Mn3O4-based nanocomposites in removal of methyl orange. *Materials Chemistry and Physics*, *239*, 122108. https://doi.org/10.1016/j.matchemphys.2019.122108

32 Pancha, I., Chokshi, K., Ghosh, T., Paliwal, C., Maurya, R., Mishra, S., 2015. Bicarbonate supplementation enhanced biofuel production potential as well as nutritional stress mitigation in the microalgae *Scenedesmus* sp. CCNM 1077. Bioresour Technol 193, 315–323. https://doi.org/10.1016/j.biortech.2015.06.107

33 Piaskowski, K., □ widerska-D□ browska, R., Zarzycki, P.K., 2018. Dye Removal from Water and Wastewater Using Various Physical, Chemical, and Biological Processes. J AOAC Int 101, 1371–1384. https://doi.org/10.5740/jaoacint.18-0051

34 Pillai, J., 2017. Optimization of Process Conditions for Effective Degradation of Azo Blue Dye by *Streptomyces* DJP15. J Pure Appl Microbiol 11, 1757–1765. https://doi.org/10.22207/JPAM.11.4.14

35 Saket, P., Kashyap, M., Bala, K., Joshi, A., 2022. Microalgae and bio-polymeric adsorbents: an integrative approach giving new directions to wastewater treatment. Int J Phytoremediation 24, 536–556. https://doi.org/10.1080/15226514.2021.1952925

36 Salima, A., Benaouda, B., Noureddine, B., Duclaux, L., 2013. Application of *Ulva lactuca* and *Systoceira stricta* algae-based activated carbons to hazardous cationic dyes removal from industrial effluents. Water Res 47, 3375–3388. https://doi.org/10.1016/j.watres.2013.03.038

37 Samchetshabam, Gita, Hussan Ajmal, Choudhury. T. G., 2017. Impact of textile dyes waste on aquatic environments and its treatment. Environ. Ecol, 35(3C), pp.2349-2353.

38 Sarkar, S., Banerjee, A., Halder, U., Biswas, R., Bandopadhyay, R., 2017. Degradation of Synthetic Azo Dyes of Textile Industry: a Sustainable Approach Using Microbial Enzymes. Water Conserv. Sci. Eng. 2, 121–131. https://doi.org/10.1007/s41101-017-0031-5

39 Silverstein, R.W., Bassler, G.C., 1963. Spectrometric Identification of Organic Compounds. J Med Chem 6, 826–827.

40 Tripathi, R., Singh, J., & Thakur, I. S. (2015). Characterization of microalga Scenedesmus sp. ISTGA1 for potential CO2 sequestration and biodiesel production. *Renewable Energy*, *74*, 774–781. https://doi.org/10.1016/j.renene.2014.09.005

41 Wu, K., Pan, X., Zhang, J., Zhang, X., Salah zene, A., Tian, Y., 2020.

Biosorption of Congo Red from Aqueous Solutions Based on Self-Immobilized Mycelial Pellets: Kinetics, Isotherms, and Thermodynamic Studies. ACS Omega 5, 24601–24612. https://doi.org/10.1021/acsomega.0c03114

42. Yan, H., Pan, G., 2004. Increase in biodegradation of dimethyl phthalate by *Closterium lunula* using inorganic carbon. Chemosphere 55, 1281–1285. https://doi.org/10.1016/j.chemosphere.2003.12.019